Motion mitigation for lung cancer patients treated with active scanning proton therapy

Clemens Grassberger[a)]
Department of Radiation Oncology, Massachusetts General Hospital and Harvard Medical School, Boston, Massachusetts 02114 and Center for Proton Radiotherapy, Paul Scherrer Institute, Villigen-PSI 5232, Switzerland

Stephen Dowdell, Greg Sharp, and Harald Paganetti
Department of Radiation Oncology, Massachusetts General Hospital and Harvard Medical School, Boston, Massachusetts 02114

(Received 29 July 2014; revised 16 February 2015; accepted for publication 17 March 2015; published 21 April 2015)

Purpose: Motion interplay can affect the tumor dose in scanned proton beam therapy. This study assesses the ability of rescanning and gating to mitigate interplay effects during lung treatments.
Methods: The treatments of five lung cancer patients [48 Gy(RBE)/4*fx*] with varying tumor size (21.1–82.3 cm^3) and motion amplitude (2.9–30.6 mm) were simulated employing 4D Monte Carlo. The authors investigated two spot sizes ($\sigma \sim 12$ and ~3 mm), three rescanning techniques (layered, volumetric, breath-sampled volumetric) and respiratory gating with a 30% duty cycle.
Results: For 4/5 patients, layered rescanning 6/2 times (for the small/large spot size) maintains equivalent uniform dose within the target >98% for a single fraction. Breath sampling the timing of rescanning is ~2 times more effective than the same number of continuous rescans. Volumetric rescanning is sensitive to synchronization effects, which was observed in 3/5 patients, though not for layered rescanning. For the large spot size, rescanning compared favorably with gating in terms of time requirements, i.e., 2*x*-rescanning is on average a factor ~2.6 faster than gating for this scenario. For the small spot size however, 6*x*-rescanning takes on average 65% longer compared to gating. Rescanning has no effect on normal lung V_{20} and mean lung dose (MLD), though it reduces the maximum lung dose by on average $6.9 \pm 2.4/16.7 \pm 12.2$ Gy(RBE) for the large and small spot sizes, respectively. Gating leads to a similar reduction in maximum dose and additionally reduces V_{20} and MLD. Breath-sampled rescanning is most successful in reducing the maximum dose to the normal lung.
Conclusions: Both rescanning (2–6 times, depending on the beam size) as well as gating was able to mitigate interplay effects in the target for 4/5 patients studied. Layered rescanning is superior to volumetric rescanning, as the latter suffers from synchronization effects in 3/5 patients studied. Gating minimizes the irradiated volume of normal lung more efficiently, while breath-sampled rescanning is superior in reducing maximum doses to organs at risk. © *2015 American Association of Physicists in Medicine.* [http://dx.doi.org/10.1118/1.4916662]

Key words: lung cancer, motion mitigation, active scanning proton therapy, interplay effect

1. INTRODUCTION

Over the past decade, there have been significant improvements in the management of lung cancer with radiotherapy. However, both non-small cell (NSCLC) and small cell lung cancer (SCLC) carry a dire prognosis if not detected at an early stage of disease.[1] Retrospective analyses have found a steep dose-response relationship in stages I–III lung cancer,[2] though toxicity concerns limit the dose that can be delivered safely with concurrent chemotherapy.[3]

Active scanning proton therapy has the potential to allow dose escalation compared to passively scattered protons or intensity-modulated radiotherapy with photons.[4] In active scanning, a narrow beam of protons is employed to scan the target in 3D, allowing the creation of inhomogeneous fields and boosting of subvolumes.[5] However, for moving tumors the dose distribution can be affected by interference between the dynamic pencil beam delivery and tumor motion, referred to as *interplay effect*, which has been the subject of recent studies.[6–8]

Though it has been shown that the averaging effect over many fractions in a conventional treatment schedule can mitigate the interplay effect,[8] this does not extend to hypofractionated treatment schedules that are currently being investigated (e.g., NCT01770418, clinicaltrials.gov). This study investigates mitigation techniques to reduce the interplay effect in these cases.

Applying state-of-the-art 4D Monte Carlo simulations and deformable image registration techniques to account for the challenging environment for dose calculation,[9] the following questions are addressed:

1. How many rescans are required to maintain target coverage (i.e., >98% of the prescribed dose) and how big is the influence of the spot size on rescanning?

2. How does volumetric rescanning (VR) compare to layered rescanning (LR)?
3. How well do methods that require coordination of breathing phase and beam delivery (i.e., breath-sampled rescanning and gating) mitigate the interplay effect compared to continuous rescanning?
4. What is the impact of the various motion mitigation techniques on the dose to the normal lung?

2. MATERIALS AND METHODS

2.A. Patient cohort and treatment planning

Five patients who have exhibited considerable degradation of the dose distribution due to interplay effects[8] are included in this investigation. The selected cases represent a range of tumor sizes, locations, and peak-to-peak motion amplitudes, as shown in Table I.

Volume definitions, constraints, and treatment planning are based on clinical trial guidelines (ClinicalTrials.gov ID: NCT00495040). The internal gross tumor volume (IGTV) is contoured on the maximum-intensity projection CT, and the 4D-CT is used to ensure that it covers the target in each phase. An 8-mm isotropic extension of the gross tumor volume (GTV) is defined as clinical target volume (CTV) to account for microscopic disease spread, and the internal clinical target volume (ICTV) covers the CTV in each phase of the breathing cycle. Contours are subsequently transferred to the average-intensity projection CT with the IGTV volume set to a generic tumor density (HU = 50). Previous studies[10] have shown that this approach provides acceptable tumor-coverage, while minimizing treatment uncertainties and dose to normal tissue.

Treatment plans are optimized using the Astroid[11] system for proton beam scanning with a prescription dose of 48 Gy(RBE) administered in four fractions in accordance with an open protocol at our institution. All plans were optimized employing two coplanar fields with the in-field inhomogeneity restricted to ≤20%. The plans delivered the prescribed dose to >99% of the ICTV and satisfied all clinical normal tissue constraints.[12]

2.B. Monte Carlo simulations of the active scanning delivery system

We simulate a scanning system based on the proton center at Massachusetts General Hospital, employing two different spot sizes that represent the extremes currently used in proton therapy centers: the big spots (bigSpots) and small spots (smallSpots) sigma vary between 8–17 mm and 2–4 mm, respectively, in the energy range 70–230 MeV.[13] The spacing in between the spots was set to 1 sigma, i.e., it varied between the spot sizes and among the energy layers. The energy switching time of the scanning system is assumed to be 1 s, the x/y scanning speeds 3/30 m/s, the spot settling time 10 ms, and the beam current 2 nA, representative for many operating proton facilities. The breathing period was assumed to be 5 s, and all treatment plans consisted of 12–15 energy layers per field with approximately 500 and 10 000 spots in each field for the large and small spot sizes, respectively (see Table I). Only the fields for patient 3 incorporated ~1000 and 20 000 spots for the large and small spot sizes, respectively, because of the large tumor volume. Previous work has shown how the interplay effect changes when beam delivery and treatment plan parameters are varied.[14]

We use TOPAS, an extensively tested Monte Carlo toolkit,[15] for all simulations. To simulate the breathing motion of the patient during treatment, we employ Plastimatch (plastimatch.org) to register the dose delivered in each phase back to the reference phase ($T50$ = end-exhale).

2.C. Data metrics and statistical tests used for analysis

We use equivalent uniform dose (EUD, $a = -20$), the dose to 99% of the target (D_{99}), and D_{5-95} (a measure of dose inhomogeneity[6]) as metrics to analyze the resulting dose distribution within the target. For the dose distribution in normal lung (defined as combined lungs minus IGTV), we use V_{20}, mean lung dose (MLD), and maximum dose for analysis.

The statistical analysis is tailored to the limited number of patients under investigation and seeks to find parameters that have a statistically significant correlation to draw valid

TABLE I. Patient characteristics: tumor size, location, motion amplitude, and plan characteristics, i.e., number of energy layers and spots per field. The tumor location is encoded as $(R/L)(L/M/U)(L)$ = (Right/Left) (Lower/Medium/Upper) (Lobe).

					No. of Energy layers/No. of spots	
Patient Nr	Tumor size (cm^3)	Location	Motion (mm)	Spot size	Field 1	Field 2
1	21.1	*RLL*	30.6	BigSpots	14/464	12/558
				SmallSpots	14/9890	12/11 400
2	26.0	*LLL*	10.7	BigSpots	14/510	12/540
				SmallSpots	14/10 290	12/10 611
3	82.3	*RUL*	20.2	BigSpots	14/994	14/1024
				SmallSpots	15/20 614	14/21 312
4	24.5	*RML*	9.1	BigSpots	14/670	14/647
				SmallSpots	14/13 384	14/12 921
5	33.9	*RUL*	2.9	BigSpots	12/575	13/611
				SmallSpots	13/11 826	13/12 797

conclusions. To explicitly state which conclusions can and cannot be drawn from our results, we divide them in three categories that we reiterate in Sec. 5.

As the initial breathing phase, i.e., the phase in which the treatment starts, has an impact on the result,[6–8] we simulate four equally spaced initial breathing phases for each patient and motion mitigation scenario. The student's t-test is used to test if results are significantly different from the planned values. This implies that the values resulting from different initial breathing starting phases are normally distributed, which in our experience is a valid assumption. To perform the statistical analyses, we use MATLAB (v2014a, The Mathworks, Inc.), its statistics toolbox (v9.0), and R (v3.1.2, R Foundation for Statistical Computing).

2.D. Motion mitigation techniques

To mitigate the interplay effect, we investigate several techniques: volumetric, layered and breath-sampled rescanning, and gating. In rescanning,[16] the dose is delivered in n scans with $1/n$ of the original spot weight to mitigate the interplay effect through statistical averaging. In *volumetric* rescanning, the whole volume is scanned at once and the rescans are applied continuously, i.e., the system starts the next scan as soon as the last scan has finished. In *layered* rescanning, each energy layer is rescanned continuously to the prescribed dose before moving to the next energy. In breath-sampled rescanning (BS rescanning), the volumetric rescans are not executed continuously, but evenly spaced in time over the breathing cycle.[17] Volumetric and layered rescannings are investigated up to ten rescans while breath-sampled is applied up to four rescans. For gating, we use a duty cycle of 30% over the T40-50-60 phases around end-exhale (T50). For these treatments, the contours and CT are modified to only include these three phases and the treatment plans are altered accordingly.

3. RESULTS

3.A. Effect of motion mitigation on the dose distribution in a tumor

Figure 1 demonstrates the effects of the various rescanning methods on the delivered dose distribution. Figure 1(A) shows a transverse slice through the IGTV after just one scan, i.e., without any motion mitigation, revealing underdosage by as much as 30% of the prescribed dose. Different rescanning methods [Figs. 1(B)–1(D)] improve the dose distribution, while gating [1(E)] results in a very homogeneous target dose.

Figure 2 shows the impact of the analyzed motion mitigation techniques on the interplay effect in the CTV for one example patient: EUD is shown on the left, D_{99} in the middle, and D_{5-95} on the right. The values in the EUD and D_{99} graphs are percentages of the planned values to avoid any bias due to differences in plan quality.

For each continuous rescanning technique, i.e., volumetric and layered, four different starting phases were simulated to determine the variation in the interplay effect based on the initial phase, i.e., treatment starting at T0 (peak inhale), T25 (midexhale), T50 (end-exhale), and T75 (midinhale). Previous studies have shown the interplay effect to vary extensively with the initial breathing phase.[7,8,14] The values shown for rescanning are the averages of these four initial breathing phases that were simulated; the error bars visualize the variability of the effect due to the dependence on the exact starting phase. As the breathing phase is controlled in breath-

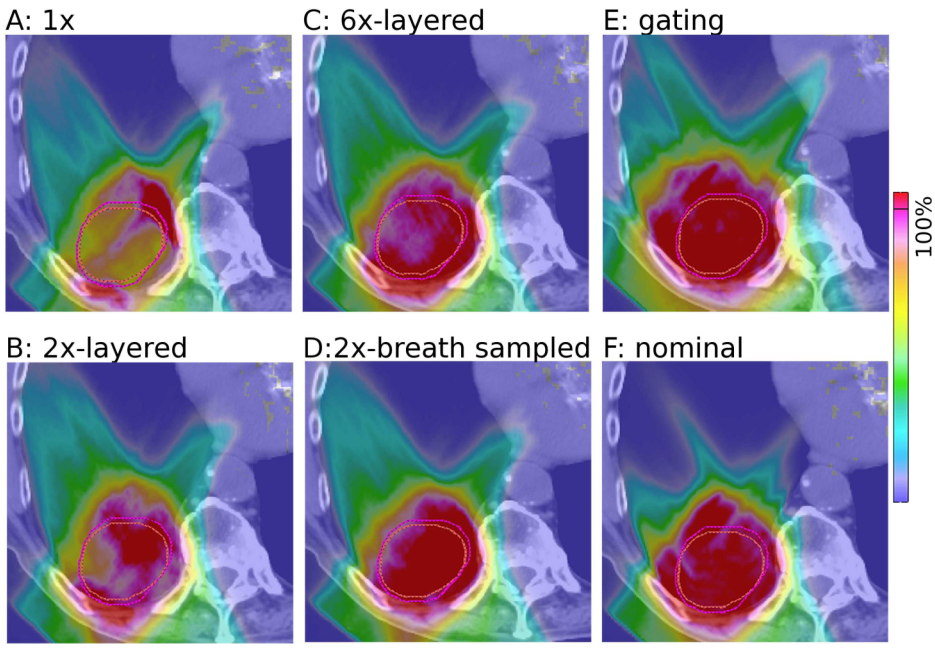

FIG. 1. Transverse slice of patient 1 after 4D-simulation of a single fraction for different motion mitigation approaches: (A) no motion mitigation, (B) 2x-layered rescanning, (C) 6x-layered rescanning, (D) 2x breath-sampled rescanning, and gating (E). (F) shows the nominal, i.e., expected, distribution without any motion, simulated on the planning CT. The color bar is in percent of prescribed dose, the contours represent the GTV (orange/inner contour), and the IGTV (magenta/outer contour).

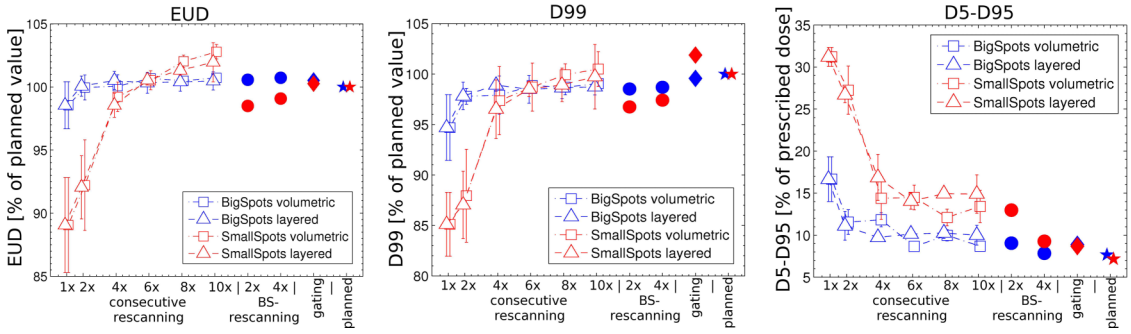

FIG. 2. Results for the CTV of patient 3: EUD (left), D_{99} (middle), and D_{5-95} (right). Triangles, layered rescanning; squares, volumetric rescanning; circles, breath-sampled rescanning (BS-rescanning); and diamonds, gating. The values for EUD and D_{99} are relative to the planned dose distribution (=stars). Error bars represent the standard deviation from the four starting phases studied for each rescanning setting. Layered and volumetric symbols have been slightly offset to ease differentiation, lines connect data points to guide the eye.

sampled rescanning and gating, these values do not have this variability.

Volumetric and layered rescannings mitigate motion equally well for this patient, i.e., $2x$-rescanning is sufficient for the large spot size (big spots), while $6x$-rescanning is necessary for the smaller spot size (small spots). Breath-sampling the timing of the rescanning proves to be more efficient by a factor of ~2 compared to continuous rescanning for this patient.

Table II shows the EUD values for all patients and scenarios considered. The standard deviation for the rescanning value represents the spread among different starting phases; stars designate significant difference from the planned EUD value. Bold numbers indicate the lowest number of rescannings at which the EUD is *both* not significantly different from the planned value and >98% of the planned EUD, meaning that the interplay effect was successfully mitigated. Usually, these two conditions coincide, only for patient 2 and $4x$-rescanning,

TABLE II. EUD values of all patients for the large spot size (top) and the small spot size (bottom). All values are in percent of the EUD in the static plan. The values for continuous rescanning are the averages of four different starting phases and the standard deviation represents the spread among these values. (a) indicate that the value for this number of rescannings is significantly lower than the static value at two different significance levels (a/b: $\rho < 0.05/0.01$, Student's t-test). Bold numbers indicate the lowest number of rescannings at which the value is *both* not significantly different from the planned value and >98% of the planned EUD. (d) indicate that layered rescanning is significantly better than volumetric rescanning (d: $\rho < 0.05$, Student's t-test, patient 2, $4x$-rescanning is a borderline case with $p = 0.062$). (c) indicate that this number of breath-sampled rescannings is significantly better than the same number of continuous rescannings (c: $\rho < 0.05$, Student's t-test).

			Continuous rescanning					Breath-sampled rescanning		
Patient	No. of rescanning	Type	$2x$	$4x$	$6x$	$8x$	$10x$	$2x$	$4x$	Gating
Big spots										
1	91.2	Layer	91.9±5.5	94.2±3.2[a]	94.6±0.5[b]	94.7±2.7[a]	94.5±2.1[a]	94.9	95.3	98.2
		Volume	93.9±2.7[a]	94.8±1.8[a]	94.9±1.5[b]	93.4±4.4	94.8±0.5[b]			
2	97.6	Layer	**99.3±3.0**	100.2±1.3	100.1±0.6	100.2±0.8	100.0±0.5	99.9	100.2	98.5
		Volume	**99.3±2.0**	100.1±0.5	99.8±0.7	100.1±0.5	100.0±0.2			
3	98.55	Layer	**100.1±0.8**	100.5±0.7	100.3±0.8	100.4±0.7	100.5±0.7	100.6	100.7	100.5
		Volume	**100.0±1.0**	100.1±0.9	100.7±0.1	100.5±0.4	100.7±0.1			
4	100.1	Layer	**101.1±0.4**	101.1±0.5	101.3±0.2	101.3±0.4	101.4±0.2	101.3	101.4	99.3
		Volume	**100.9±0.3**	101.3±0.1	101.3±0.0	101.3±0.2	101.1±0.5			
5	99.38	Layer	**99.9±1.1**	100.0±0.6	100.1±0.2	100.2±0.1	100.2±0.2	100.2	100.3	101.3
		Volume	**99.9±0.4**	100.2±0.2	100.2±0.1	100.1±0.1	100.2±0.1			
Small spots										
1	61.1	Layer	78.38±5.0[b,d]	84.04±4.4[b]	85.95±1.8[b]	86.61±2.1[b,d]	87.32±1.0[b]	83.1[c]	86.75	93.1
		Volume	69.03±7.3[b]	78.94±6.0[b]	82.55±5.1[b]	78.91±4.2[b]	87.22±0.4[b]			
2	89.16	Layer	96.79±1.4[a]	97.01±2.8	**98.93±1.8**	100.2±1.3	101.3±1.3	99.1[c]	100.5	98.8
		Volume	97.77±0.7[b]	92.39±5.3	**100.9±0.4**	101.1±0.6	100.9±1.0			
3	89.06	Layer	92.05±2.4[b]	**98.55±0.9**	100.5±0.4	101.3±0.4	102±1.5	98.5[c]	99.08	100.3
		Volume	92.22±3.5[a]	**99.22±1.1**	100.5±0.7	102±0.5	102.8±0.6			
4	93.46	Layer	**98.22±2.7**	100.2±1.4	101.5±0.8	102.1±0.9	102.8±0.3	100.4[c]	101.7	102.6
		Volume	96.89±1.7[a]	**99.17±3.3**	99.96±2.1	102.5±0.5	103.1±0.5			
5	94.94	Layer	97.34±1.0[a]	**99.3±0.6**	99.68±0.5[d]	100.7±0.4	101.1±0.5	99.71[c]	100	98.4
		Volume	96.33±1.0[b]	**100.2±0.1**	95.73±1.6[a]	100.7±0.5	101.6±0.2			

the large spread among results for the initial breathing phases causes the averages to be not significantly different from the static plan ($\rho = 0.13/0.07$ for layered/volumetric rescanning).

The planned target dose for patient 1, which shows the largest tumor motion amplitude (30.6 mm), is only successfully delivered using gating and a large spot size. Even for a large number of rescans (10x-rescanning) the EUD plateaus at ≈95% for big spots and just below ≈90% for small spots. For the small spot size, the residual motion during the gating window is apparently large enough to reduce the EUD to 93.1% of the planned value. For all other patients, the data presented in Table II show that 2x rescanning is sufficient to restore the dose for the large spot size, even for patient 3 with a motion of ≈20 mm. For the small spot size on the other hand, between two and six continuous rescannings are necessary to successfully mitigate motion effects. If BS-rescanning is used, two scans are adequate. Gating succeeds in giving a uniform target dose for all patients except for the largest motion amplitude and small spot size (patient 1). In three of the studied patients, a *synchronization effect* is observed for volumetric rescanning, where a specific number of rescans is associated with a lower EUD (patient 1 8x-, patient 2 4x-, and patient 5 6x-volumetric rescannings). This affects surfaces if the total time to scan the tumor is close to an integer multiple of the breathing period, hampering the averaging effect usually provided by rescanning. This synchronization effect is only observed for volumetric rescanning and has not been seen in layered rescanning, as the time to scan each layer is different, making synchronization of multiple layers with the breathing period is unlikely.

3.B. Effect of motion mitigation on dose distribution in normal lung

The effect of motion mitigation on the dose to the normal lung depends heavily on the quantity to be analyzed. Rescanning has a minimal effect on the V_{20} and the MLD, which stay constant with the numbers of rescanning, as can be seen in Fig. 3. The effect on the maximum dose to the normal lung is however considerable: for the large spot size, 10x-rescanning reduces the maximum dose to the lung on average by 6.9 ± 2.4 Gy(RBE), while the reduction is 16.7 ± 12.2 Gy(RBE) for the small spot size. For gating the reduction is similar, 6.8 ± 4 Gy(RBE) for the large spot size and 16.42 ± 8.4 Gy(RBE) for the small spot size. For breath-sampled rescanning, the reduction is larger, i.e., 8.0 ± 2.0/9.7 ± 2.8 Gy(RBE) for 2x/4x-rescanning for the large spot size and 17.5 ± 6.7/22.7 ± 10.3 Gy(RBE) for 2x/4x-rescanning for the small spot size, respectively.

Gating on the other hand is far more efficient in reducing the V_{20} and MLD, which can be seen in Fig. 3, because the treatment field size is being reduced. Averaged over all patients the absolute reduction in V_{20} is 1.0% ± 2.5% and 1.8% ± 2.0%, in MLD 0.5 ± 1.3 Gy(RBE) and 1.1 ± 1.2 Gy(RBE), for the large and small spot sizes, respectively. The exact reduction is patient-specific and depends on the size of the tumor and the motion amplitude. The maximum reduction observed for the considered patient population occurred in patient 3, combining a large tumor (82.3 cm^3) with extensive motion (20.2 mm). In this patient, the V_{20} and MLD are reduced by 5% and 2.5 Gy(RBE), respectively. Figure 3 also shows the generally smaller lung exposure when using a small spot size, which yields on average 6.1% ± 3.0% lower V_{20} and 3.7 ± 1.6 Gy(RBE) lower MLD values.

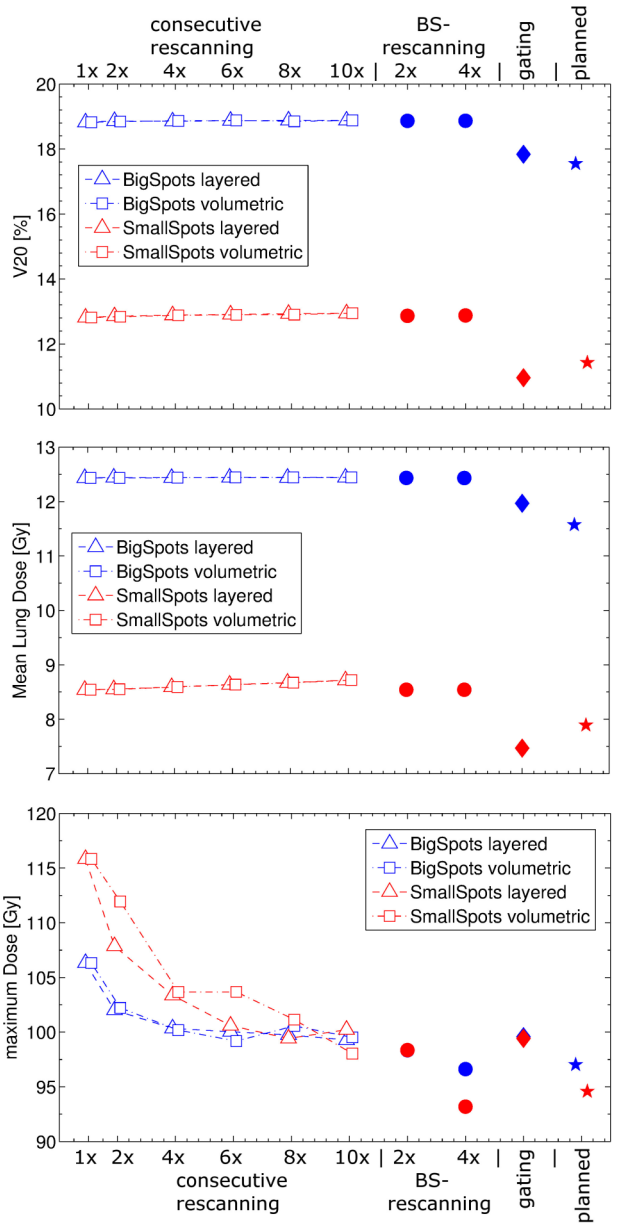

FIG. 3. Absolute values of normal lung V_{20}, mean and maximum dose averaged over all patients. Triangles, layered rescanning; squares, volumetric rescanning; circles, breath-sampled rescanning (BS-rescanning); diamonds, gating; and stars, static plan.

3.C. Time requirements of rescanning and gating

The delivery times required for the considered motion mitigation techniques are presented in Table III. The times quoted are delivery times only and do not include gantry rotation, additional imaging, patient setup, and other factors. In this study, two fields have been used for all patients, though

TABLE III. Times required for different motion mitigation techniques. LR, layered rescanning; VR, volumetric rescanning.

Patient Nr	Tumor size (cm^3)	Spot size	Scanning times (min/field) None	2x-LR	6x-LR	2x-VR	6x-VR	Gating
1	21.1	BigSpots	0.6	0.7	0.9	0.9	2.0	2.0
		SmallSpots	1.7	2.9	7.9	3.1	8.9	5.5
2	26.0	BigSpots	0.6	0.7	0.9	0.9	2.0	2.1
		SmallSpots	1.7	2.9	7.8	3.1	8.8	5.5
3	82.3	BigSpots	0.9	1.0	1.5	1.2	2.6	2.9
		SmallSpots	3.0	5.5	15.3	5.7	16.5	10.0
4	24.5	BigSpots	0.7	0.7	1.0	1.0	2.2	2.2
		SmallSpots	2.0	3.5	9.6	3.7	10.8	6.5
5	33.9	BigSpots	0.6	0.7	1.0	0.9	2.0	2.1
		SmallSpots	1.9	3.3	9.1	3.5	10.1	6.1

in the clinic, we employ up to four fields, depending on the complexity of the case.

Rescanning two times with the large spot size, which is required to maintain the planned dose in the target, is a factor of 3.0/2.3 (layered/volumetric) faster than gating with a 30% duty cycle. For the small spot size however, rescanning six times is required to maintain the planned dose, which takes a factor of 1.5/1.7 (layered/volumetric) longer than gating for this scenario.

Table III also demonstrates the effect the spot size has on the treatment time. Without any motion mitigation technique, the large spot size takes approximately a factor of ~2.9 less time than the small spot size to deliver a field. For 2x-rescanning, the larger spot size will deliver the field a factor of 4.7/3.9 (layered/volumetric) faster than the smaller one. For 6x-rescanning, this differential increases further to 9.3/5.1 for layered/volumetric rescanning, respectively. Thus, the spot size impacts the treatment time comparatively more for layered rescanning and increases with the number of rescans.

4. DISCUSSION

For four out of five patients investigated in this study, rescanning can retain the EUD > 98% of the prescribed dose. The tumor motion amplitude of these four patients ranges from 3 to 20 mm. The number of required rescannings for these four patients is relatively low, i.e., up to two for the large spot size and up to six for the small spot size considered. Previous studies have demonstrated that the magnitude of the interplay effect is very patient-specific and cannot be predicted by the tumor motion amplitude.[7,8] Hence, the required number of rescannings for a given patient is hard to predict, as even patients with considerable motion of 15 mm do not necessarily exhibit dose degradation through interplay (e.g., patients 5 and 8 in Ref. 8).

In three out of the five patients studied, the efficacy of volumetric rescanning is compromised by a *synchronization effect* between the time to scan the tumor and the breathing period. As the total dose deposited per scanning changes with the number of rescannings and influences the total time to scan, this effect usually surfaces only for a specific number of rescannings. Figure 4 demonstrates this effect for patient 2: for 4x volumetric rescanning with the small spot size, the EUD is greatly reduced, almost to the level of no motion mitigation, while layered rescanning is not affected. This advantage of layered rescanning has recently also been demonstrated by Bernatowicz *et al.*, who observed higher fluctuations in volumetric compared to layered rescanning in two liver patients.[18]

For more than 6x-rescanning, the EUD in Fig. 2 becomes higher than the nominal value, which has also been observed by other authors for liver cases.[6] The reason for this is that rescanning can average out hot- and cold spots that were present in the static dose distribution, making the delivered dose distribution *more homogeneous* compared to the planned dose.

Breath-sampling rescanning has been shown to be highly effective in overcoming the synchronization effect. It also renders rescanning more effective. As shown in Table II,

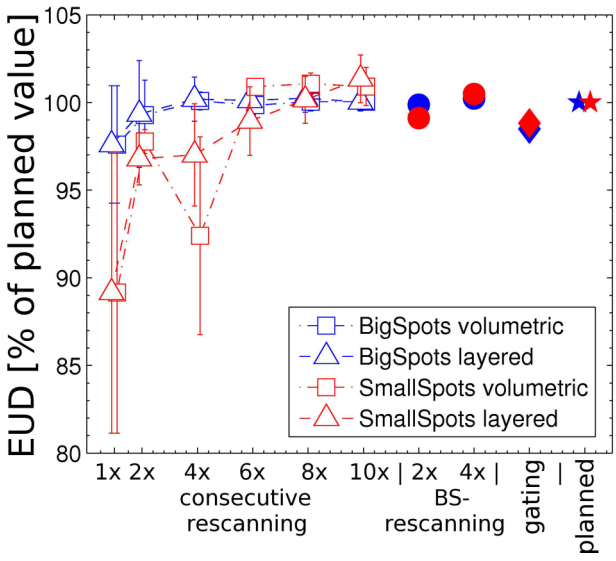

FIG. 4. Example of a synchronization effects in patient 2 as shown by the increase in the interplay effect for 4x volumetric rescanning. Triangles denote layered rescanning, squares volumetric rescanning, circles breath-sampled rescanning (BS-rescanning), and diamonds gating. Values are relative to the planned dose distribution. Error bars represent the standard deviation from the four starting phases studied for each rescanning setting. Layered and volumetric symbols have been slightly offset to ease differentiation.

volumetric rescanning twice starting half a breathing period apart is as efficient as 4–6 continuous rescans, depending on the patient. For all patients under investigation, 2x-breath-sampled rescanning is significantly better than 2x-continuous rescanning for the small spot size. For the large spot size, this effect is not visible, as 2x-continuous rescanning is already effectively mitigating the interplay effect.

Furthermore, the results have shown that gating with a 30% duty cycle is a valid option for four of the five patients in the investigated cohort. For the largest motion amplitude however, gating can only restore the EUD to >98% of the prescribed value for the large spot size. For the small spot size, the residual motion in the gating window is apparently still considerable, which would warrant further countermeasures. Restriction of the gating window is possible, but in this case, time delays[19] and the performance of the motion monitoring itself become critical, requiring accuracy of the order of ≈1 mm.[20] Another option would be to combine gating with rescanning, which would lead to further lengthening of the treatment time.[21]

The time structure of the simulated scanned beam delivery was based on the system at the Francis H Burr proton therapy center at MGH. However, many proton centers feature similar technical parameters to the ones studied here (see Sec. 2.A). The considered spot sizes include the two extremes of the scanning systems currently in operation. Thus, our conclusions hold for a wide range of proton centers. Note also that the interplay effect does not vary substantially with the parameters of the scanning system other than the spot size.[14] If the number of rescans becomes very large, the requirement for the number of protons per spot could be below the limits of deliverability. This has not impacted this study because of the investigation of large fraction sizes (12 Gy/fraction) and relatively low numbers of rescanning (up to $n = 10$).

All treatment plans in this study have been based on pretreatment 4D-CT scans of the patients, and its results are based on the validity of the anatomy and positioning for the time of treatment. It has been shown[22] that tumor trajectory and position can vary in between fractions, highlighting the need for daily image-guidance when treating lung cancer with protons. Additionally, we used the concept of a geometrical ITV with a density override, as specified in a current clinical trial protocol (see Sec. 2). Knopf *et al.*[23] have compared a purely geometrical ITV approach *without* density override to a range-adapted ITV approach and have seen differences in the lung case they studied. For patient 1, where rescanning is not able to mitigate the dose degradation, it is possible that other planning approaches yield more promising results.

Regarding dose to normal tissue, breath-sampled rescanning is more effective in reducing the maximum dose to the lung (or other tissues located distal to the target), while gating can also reduce the V_{20} and MLD through the reduction of the treatment field. As the latter quantities are more suitable proxies to estimate the incidence of severe lung complications such as radiation pneumonitis,[12] gating is allegedly superior to rescanning regarding lung side effects. The exception might be cases in which critical structures sensitive to the maximum dose, such as spinal cord, esophagus, and to some extent the heart, are located behind the distal edge of the beam. In this case, breath-sampled rescanning could be necessary to reduce the impact of hotspots, possibly in addition to gating.

The time required for the motion mitigation techniques studied depends heavily on the spot size, as can be seen in Table I. This is because some processes, for example, the spot settling time (e.g., 10 ms/spot in our case) scale linearly with the number of spots in the field. This leads to the large observed increase in treatment time for layered rescanning with the small spot size, as the number of spots is a factor of ∼15 higher, as a smaller spot size warrants smaller lateral distances between spots (spacing between spots in this work is 1 sigma).

Generally, layered rescanning has the advantage of being faster than volumetric rescanning, but this advantage decreases comparatively with the smaller spot size, as the time it takes to switch between energy layers is no longer a considerable fraction of the treatment time. This leads to the conclusion that the largest gains in treatment time can be obtained through faster in-layer scanning, not faster energy switching, as layered rescanning is the more robust option compared to volumetric rescanning. The results regarding the time requirements are naturally dependent on the exact scanning system in use, especially on the in-layer scanning speed and energy switching time. However, the parameters we use here are similar to many scanning systems in use and under construction so can be considered representative for the majority of proton therapy centers.

5. CONCLUSION

To explicitly state which conclusions can be drawn from our results and which ones can not, we have categorized them into three classes.

5.A. Conclusions that are generally applicable beyond this patient cohort

- **Layered vs volumetric rescanning:** Layered rescanning performed similar to volumetric rescanning in all patients and scenarios studied. However, in three out of the five patients under investigation volumetric rescanning performed significantly worse for a specific number of rescans due to synchronization effects.
- **Breath-sampling:** Breath-sampled rescanning is significantly better than continuous rescanning for two repaintings, reducing underdosage due to interplay by a factor of ∼2.
- **Time requirements:** Layered rescanning is faster than volumetric rescanning, though the advantage decreases for small spot sizes. As it is also more robust (as mentioned above), future developments in proton gantry and beam-line design to treat moving targets should focus primarily on fast in-layer delivery times, i.e., magnet speed and beam current, rather than fast energy switching times.
- **Normal lung:** Gating minimizes the dose to normal lung, though if the maximum dose to critical structures

is important, breath-sampled rescanning outperforms gating especially for small spot sizes. Thus, if critical organs such as the esophagus, spinal cord, or heart is located at the distal edge of a field, breath-sampling rescanning might be advantageous, potentially in combination with gating.

5.B. Conclusions that are applicable to the patients under investigation

— Rescanning 2–6 times (depending on spot size) was able to mitigate the interplay effect completely in the four patients with motion amplitudes up to 20 mm. However, this conclusion cannot be extended to other patients not included in this study.
— Rescanning was not able to mitigate the interplay effect for the patient with 30 mm motion. However, it is not clear if this indicates a general inability of rescanning to deal with very large motion amplitudes, or if this is related to the exact planning technique, as discussed above.
— Gating was able to mitigate the interplay effect completely in all five patients for the large spot size and in 4/5 for the small one. This cannot be extended to a general patient population.

5.C. Conclusions that cannot be drawn from this data set

— It cannot be generally predicted how many rescannings are necessary for a specific patient with a given motion amplitude. This is inherent in the patient-specific nature of the interplay effect, as the dose degradation does not correlate well with motion amplitude.[6–8]

This last observation implies that question No. 1 posed in the Introduction cannot be answered for a specific patient. This reflects the authors' view that the interplay effect and its mitigation are inherently patient-specific phenomena, which have to be studied in actual patients. However, the authors are confident that a threshold, i.e., a specific number of rescans that mitigates the interplay effect in the overwhelming majority of patients, exists and can be found.

ACKNOWLEDGMENTS

The authors would like to acknowledge Dr. Anthony Lomax for improving this paper through lively discussion, Dr. Brian Healy for his insights into statistics, Dr. Ben Clasie for sharing his knowledge about active scanning proton delivery systems, Dr. Henning Willers for fruitful discussions concerning clinical relevance, and Dr. Jon Jackson and Partners Research Computing for maintenance of the computing cluster. This work was supported by the National Cancer Institute under R01CA111590. The authors report no conflicts of interest in conducting the research.

[a]Author to whom correspondence should be addressed. Electronic mail: Grassberger.Clemens@mgh.harvard.edu; Telephone: +1-617-724-1202; Fax: +1-617-724-0368.

[1]D. De, W. Ruysscher, P. van Elmpt, and Lambin, "Radiotherapy with curative intent for lung cancer: A continuing success story," Radiother. Oncol. **101**(2), 237–239 (2011).
[2]M. Partridge, M. Ramos, A. Sardaro, and M. Brada, "Dose escalation for non-small cell lung cancer: Analysis and modelling of published literature," Radiother. Oncol. **99**(1), 6–11 (2011).
[3]S. E. Schild *et al.*, "Results of a phase I trial of concurrent chemotherapy and escalating doses of radiation for unresectable non-small-cell lung cancer," Int. J. Radiat. Oncol., Biol., Phys. **65**(4), 1106–1111 (2006).
[4]X. Zhang *et al.*, "Intensity-modulated proton therapy reduces the dose to normal tissue compared with intensity-modulated radiation therapy or passive scattering proton therapy and enables individualized radical radiotherapy for extensive stage IIIB non-small-cell lung cancer: A virtual clinical study," Int. J. Radiat. Oncol., Biol., Phys. **77**(2), 357–366 (2010).
[5]N. Bassler, O. Jäkel, C. S. Søndergaard, and J. B. Petersen, "Dose- and LET-painting with particle therapy," Acta Oncol. **49**(7), 1170–1176 (2010).
[6]A.-C. Knopf, T. S. Hong, and A. Lomax, "Scanned proton radiotherapy for mobile targets-the effectiveness of re-scanning in the context of different treatment planning approaches and for different motion characteristics," Phys. Med. Biol. **56**(22), 7257–7271 (2011).
[7]C. Bert, S. O. Grozinger, and E. Rietzel, "Quantification of interplay effects of scanned particle beams and moving targets," Phys. Med. Biol. **53**(9), 2253–2265 (2008).
[8]C. Grassberger *et al.*, "Motion interplay as a function of patient parameters and spot size in spot scanning proton therapy for lung cancer," Int. J. Radiat. Oncol., Biol., Phys. **86**(2), 380–386 (2013).
[9]C. Grassberger, J. Daartz, S. Dowdell, T. Ruggieri, G. Sharp, and H. Paganetti, "Quantification of proton dose calculation accuracy in the lung," Int. J. Radiat. Oncol., Biol., Phys. **89**(2), 424–430 (2014).
[10]Y. Kang *et al.*, "4D proton treatment planning strategy for mobile lung tumors," Int. J. Radiat. Oncol., Biol., Phys. **67**(3), 906–914 (2007).
[11]H. M. Kooy *et al.*, "A case study in proton pencil-beam scanning delivery," Int. J. Radiat. Oncol., Biol., Phys. **76**(2), 624–630 (2010).
[12]L. B. Marks *et al.*, "Radiation dose-volume effects in the lung," Int. J. Radiat. Oncol., Biol., Phys. **76**(3), S70–S76 (2010).
[13]E. Pedroni, D. Meer, C. Bula, S. Safai, and S. Zenklusen, "Pencil beam characteristics of the next-generation proton scanning gantry of PSI: Design issues and initial commissioning results," Eur. Phys. J. Plus **126**(7), 1–27 (2011).
[14]S. Dowdell, C. Grassberger, G. C. Sharp, and H. Paganetti, "Interplay effects in proton scanning for lung: A 4D Monte Carlo study assessing the impact of tumor and beam delivery parameters," Phys. Med. Biol. **58**(12), 4137–4156 (2013).
[15]J. Perl, J. Shin, J. Schümann, B. Faddegon, and H. Paganetti, "TOPAS: An innovative proton Monte Carlo platform for research and clinical applications," Med. Phys. **39**(11), 6818–6837 (2012).
[16]M. H. Phillips, E. Pedroni, H. Blattmann, T. Boehringer, A. Coray, and S. Scheib, "Effects of respiratory motion on dose uniformity with a charged particle scanning method," Phys. Med. Biol. **37**(1), 223–234 (1992).
[17]J. Seco, D. Robertson, A. Trofimov, and H. Paganetti, "Breathing interplay effects during proton beam scanning: Simulation and statistical analysis," Phys. Med. Biol. **54**(14), N283–N294 (2009).
[18]K. Bernatowicz, A. J. Lomax, and A. Knopf, "Comparative study of layered and volumetric rescanning for different scanning speeds of proton beam in liver patients," Phys. Med. Biol. **58**(22), 7905–7920 (2013).
[19]H.-M. Lu *et al.*, "A respiratory-gated treatment system for proton therapy," Med. Phys. **34**(8), 3273–3278 (2007).
[20]E. Rietzel and C. Bert, "Respiratory motion management in particle therapy," Med. Phys. **37**, 449–460 (2010).
[21]T. Furukawa *et al.*, "Moving target irradiation with fast rescanning and gating in particle therapy," Med. Phys. **37**(9), 4874–4879 (2010).
[22]J.-J. Sonke, J. Lebesque, and M. van Herk, "Variability of four-dimensional computed tomography patient models," Int. J. Radiat. Oncol., Biol., Phys. **70**(2), 590–598 (2008).
[23]A.-C. Knopf, D. Boye, A. Lomax, and S. Mori, "Adequate margin definition for scanned particle therapy in the incidence of intrafractional motion," Phys. Med. Biol. **58**(17), 6079–6094 (2013).